PCCP

Accepted Manuscript

ROYAL SOCIETY OF CHEMISTRY

www.rsc.org/pccp

Cite this: DOI: 10.1039/c0xx00000x

www.rsc.org/xxxxxx

ARTICLE TYPE

Electronic transport, transition-voltage spectroscopy, and Fano effect in single molecule junctions composed of biphenyl molecule attached to metallic and semiconducting carbon nanotubes electrodes

Carlos Alberto Brito da Silva Júnior[a], José Fernando Pereira Leal[b,c], Vicente Ferrer Pureza Aleixo[d], Felipe A. Pinheiro[e] and Jordan Del Nero*[f]

Received (in XXX, XXX) Xth XXXXXXXXX 20XX, Accepted Xth XXXXXXXXX 20XX
DOI: 10.1039/b000000x

We have investigated electronic transport in a single-molecule junction composed of a biphenyl molecule attached to p-doped semiconductor and metallic carbon nanotubes leads. We find that the current-voltage characteristics are asymmetric as a result of the different electronic nature of the right and left leads, which are metallic and semiconducting, respectively. We provide an analysis of transition voltage spectroscopy in such system by means of both Fowler-Nordheim and Lauritsen-Millikan plots; this analysis allows one to identify the positions of resonances and the regions where the negative differential conductance occurs. We show that transmittance curves are well described by the Fano lineshape, for both direct and reverse bias, demonstrating that the frontier molecular orbitals are effectively involved in the transport process. This result gives support to the interpretation of transition voltage spectroscopy based on the coherent transport model.

Introduction

Since the pioneer idea of a molecular rectification diode proposed by Aviram and Ratner[1], electronic transport in single molecules of the donor-bridge-acceptor type has been extensively investigated[2]. In single molecule junctions the nature of the electrodes and their connection to the molecular bridge govern electronic transport in a crucial way. Important progresses have been made in theoretical modeling electronic transport when the donor or/and acceptor are replaced by metallic or semiconducting electrodes to investigate the dependence on the bridge structure and the electronic properties of the leads[3]. The metal-molecule coupling depends on many parameters, such as the type of chemical linkage between both, the molecular conformation, and the tunneling barrier height[4,5]. For instance, the interaction between bridge and electrode is generally a weak electrostatic interaction, similar to the physisorption that occurs at many solid/gas and solid/liquid interfaces[2,6,7]. As another example, electronic conduction in metal-bridge-metal and metal-bridge-semiconductor junctions has been investigated to identify the role of molecular size and structure, as well as temperature and the magnitude of the barrier for tunneling between donor and acceptor[8]. All these factors strongly influence the current-voltage characteristics of molecular junctions, as it has been demonstrated both experimentally and theoretically[4,5].

In single-molecule junctions the so-called "alligator-clips", such as nitrogen and sulfur, are used to establish electronic contact between an inorganic electrode (*e.g.* Ag, Au, Al, Pb, Hg) and organic bridges (usually carbon atomic wires, saturated and unsaturated carbon chains). Ideally infinite carbon atomic wires are semiconducting due to Peierls distortion. However, short carbon atomic wires are usually modeled as metallic[9]. This model is justified since the energy barrier between the inorganic lead and organic bridges is typically very high, which also induces a disruption of the electronic bridge-electrode interaction[10]. The tunneling process in molecular devices is dominated by the height and width of the barrier resulting from the presence of molecules between the electrodes. The barrier height when leads are both metallic (metallic and semiconductor) is given by the energy difference between the Fermi level of the electrodes (the edge of the conduction or valence band) and the closest molecular energy levels (HOMO and/or LUMO)[11,12]. Experimentally, the connection bridge-electrode is implemented using scanning probe microscopy (SPM), scanning tunneling microscopy (STM), or conducting probe atomic force microscopy (CP-AFM) with gold tip without the presence of alligator clips[2,13-15].

Alternatively, theoretical and experimental studies on single-molecule electronic transport have revealed that junctions made of metallic carbon nanotubes (CNTs) leads offer many

[a] *Faculdade de Ciências Naturais, Universidade Federal do Pará, 68800-000, Breves, PA, Brazil.*
[b] *Pós-Graduação em Física, Universidade Federal do Pará, 66075-110, Belém, PA, Brazil.*
[c] *Departamento de Ciências Naturais, Universidade do Estado do Pará, 68745-000, Castanhal, PA, Brazil.*
[d] *Faculdade de Engenharia Elétrica, Universidade Federal do Pará, 68455-700, Tucuruí, PA, Brazil.*
[e] *Instituto de Física, Universidade Federal do Rio de Janeiro, 21941-972, Rio de Janeiro, RJ, Brazil.*
[f] *Departamento de Física, Universidade Federal do Pará, 66075-110, Belém, PA, Brazil.*

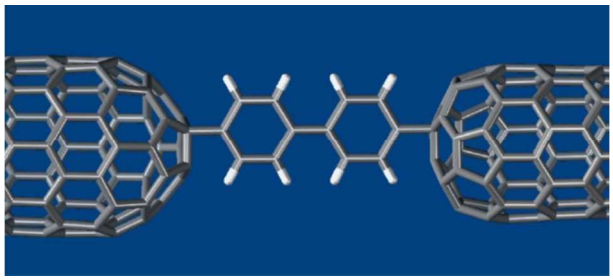

Fig. 1 Model geometry: biphenyl derivative bridging the gap between single-wall (9,0) carbon nanotube and p-doped (8,0) carbon nanotube.

advantages if compared to inorganic metallic electrodes[16-17].

Recently electronic transport and Transition Voltage Spectroscopic (TVS) have been investigated in single-molecule junctions composed of both inorganic metallic[14,15] and organic metallic leads[17]. TVS is based on the analysis of the Fowler-Nordheim plot, which exhibits a sell point V_{min}. In junctions with organic metallic leads V_{min} corresponds to voltages where negative differential resistance occurs, corroborating the coherent transport model interpretation of TVS. The fact that the metallic electrodes are made of carbon nanotubes leads to important differences in the behavior of V_{min} if compared to the case of molecular junctions with nonorganic contacts[17]. As carbon nanotubes can be either metallic or semiconductors, considering these materials as electrodes in single-molecule junctions could lead to novel electronic transport phenomena and applications. However, to the best of our knowledge this case has never been treated so far.

The aim of the present work is hence to fill this gap by investigating electronic transport and TVS in single-molecule junctions composed by metallic and semiconductor carbon nanotubes (Figure 1). We provide an analysis of TVS in such system by means of both Fowler-Nordheim and Lauritsen-Millikan plots. This analysis allows one to identify the positions of resonances and the regions where the negative differential conductance occurs. We also demonstrate that transmittance curves are well described by the Fano lineshape, for both direct and reverse bias. This result suggests that the frontier molecular orbitals are effectively involved in the transport process, corroborating the coherent transport model in single-molecule electronics and the current interpretation of TVS.

Methodology

Preceding the electronic transportation calculations, the molecular system was optimized using the B3LYP[18] level and 6-311G** basis set. The B3LYP functional has been employed to successfully describe electronic transport in single molecules attached to carbon nanotubes electrodes[17,16,19]. The relative positions of the lead carbon atoms were frozen in a typical nanotube formation as presented in Fig. 1 as well as the distance between the nanotube and phenyl rings. A full relaxation was performed during the subsequent geometric optimization.

Electronic transport calculations are grounded on the Non-Equilibrium Green's functions (NEGF) formalism coupled to *ab initio* DFT [17,20,21]. This theoretical procedure has been demonstrated to be highly reliable in predicting electronic transport properties such as current and transmission coefficients[17,19,22]. In addition, this methodology has been shown to be efficient in determining transport properties of molecular devices attached to very large electrodes[17,22].

A systematic study, with a methodology very similar to the one employed here, of electronic transport using metallic and semiconducting CNTs leads were done by Lee et al. in Ref. 23, where the presence of these electrodes gives rise to a Schottky-like behavior, depending on direction and strength of their dipole moments. Also, they investigate the possibility of controlling the I-V characteristics of these systems by manipulating the doping of the CNT units[23].

A similar DFT/NEGF[23] calculation was carried out to disclose the electrical transport properties of organic junctions connected to large reservoirs (electrodes). To compute the I-V characteristics of metallic CNT-biphenyl- p-doped semiconductor CNT, we take into account first principles methodology implemented in a FORTRAN code as previously presented [17], as well as the SIESTA package[22].

The current calculation consists of two steps: *(a)* molecular relaxation of the organic system is performed by means of quantum mechanical methodologies with specific functional and basis set (B3LYP/6-311G**). To simulate the molecular junction, each optimized molecule composed by carbon atoms of the lead were translated into a semi-infinite junction with several carbons in the surface. The supercell consists of two carbon nanotubes as the left (single wall (9,0)) and right (single wall p-doped (8,0)) layers with 184 atoms for both layers in the scattering region plus the phenyl rings as the connector between them. The molecule-organic electrode contact distance was initially set from 1.30 Å up to 1.50 Å and then optimized showing no difference in the final result. A double-ζ plus polarization basis set was used for all atoms in the organic molecule with a local density approximation in the transport calculation and norm-conserving pseudo potentials. All atoms were relaxed including optimization process resulting the force field less than 0.11 eV/Å. To achieve the self-consistency in the calculation, it is necessary to compute the charge density by integrating the contributions from scattering states between the left and right leads chemical potentials, given by the Fermi-Dirac distribution. The energy spacing around Fermi level for in/out states from bulk used in this paper are a typical 11 meV according with well-known work in the field [24] and references therein. The self-consistency is achieved after optimization of different charge densities. Before calculating the electronic current through the entire system (molecule coupled to CNTs electrodes), one should characterize the electronic properties of individual capped CNTs separately. Figure 2 reveals that the metallic and p-doped semiconductor CNTs exhibit ohmic and non-ohmic behavior, respectively. This result confirms that the CNTs can be considered bulklike and hence are adequate to be employed as electrodes in a Landauer transport calculation. As the semiconductor lead is p-doped, a narrow energy band exists in the energy region of the undoped semiconductor. The electronic transport between the leads is followed after the molecular relaxation including an applied bias between the leads and the electric signature is calculated utilizing the NEGF method.

The electronic current through the system is given by the Landauer-Büttiker formula where an integration of transmission coefficient square between the chemical potentials [25, 26, 27].

$$I = \frac{2e}{h}\int_{u_L(V_b)}^{u_R(V_b)} T\left(E,V_b\right)dE. \qquad (1)$$

The transport coefficient $T(E,V_b)$ is a function of the energy

level E at a specific bias V_b. The $u_R(V_b)$ and $u_L(V_b)$ are the energy bias region.

Electronic Transport and Transition Voltage Spectroscopy

Before the simulation of CNT p-doped (8,0) semiconductor - biphenyl – CNT (9,0) metalic junctions, we characterize the electronic transport properties of individual CNTs used as leads. In Fig. 2 the I - V (current-voltage) signature of capped CNTs,

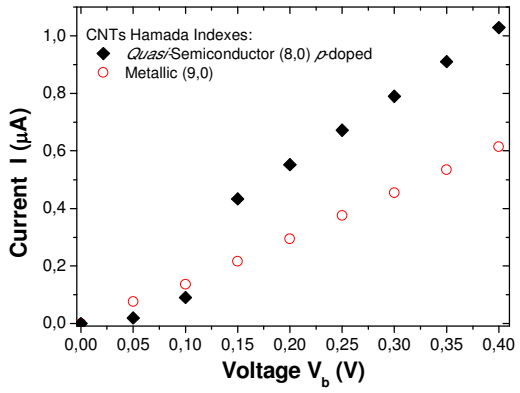

Fig. 2 (Color online) Current-Voltage feature of individual capped carbon nanotubes used as leads, calculated by means of the DFT/NEGF methodology. CNTs with Hamada indexes (8,0) (black diamonds) as quasi-semiconductor p-doped and (9,0) (open red circles) as metallic were considered.

characterized by (8,0) and (9,0) as Hamada indexes. These calculations were done by DFT/NEGF method as a function of the external bias voltage V_b revealing a typical ohmic and quasi-ohmic (non-resonant behavior) demonstrating that the (9,0) CNT is metallic and the (8,0) CNT is a p-doped semiconductor.

Also, the investigation of electrical signature for others CNTs size were performed and no qualitative differences comparing with Fig. 2 were found.

Finally, the CNTs presented in this figure can be utilized as bulk-like and they are adequate to be used as left/right leads following Landauer methodology.

Fig. 3 presents the Fowler-Nordheim (FN) plot, $\ln(I/V^2)$ versus V^{-1}, and Lauritsen-Millikan (LM) plot, $\ln(I)$ versus V^{-1} for (9,0) CNT-biphenyl– p-doped (8,0) CNT [28]. For historical reasons, it has become customary to use FN to analyze field emission current-voltage data in bulk metals. However, LM plots are in fact easier to understand and utilized in a wide range of materials. Also, LM plots are more flexible to make corrections for all physical sources of voltage dependence in the data, or to estimate uncertainties in derived parameter values when the precise forms of voltage dependences are not known[29].

The analysis of the FN and ML plots, shown in Fig. 3, reveals that there are two resonances at -0.026V and -0.236V (reverse bias), where the first corresponds to the minimum voltage (V_{min}). For forward bias two resonances occur at 0.053V and 0.184V, while one negative differential resistance (NDR) occurs at 0.367V, corresponding to a local minimum voltage (V_{min}). The LM plot shows one NDR at -0.183V that corresponds to the minimum voltage (V_{min}) for reverse bias; for forward bias there is one resonance at 0.053V (that coincides with the FN plot) and two NDRs at 0.131V and 0.367V (that coincide with the FN plot), corresponding to the minimum voltage (V_{min}).

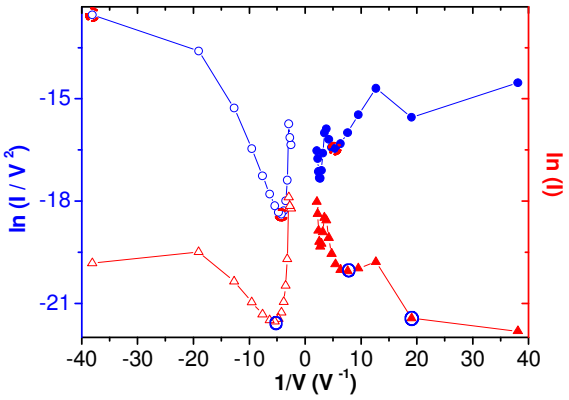

Fig. 3 (Color online): (full symbols) Forward and (open symbols) reverse bias for (blue circles) Fowler-Nordheim (FN) and (red triangle) Lauritsen-Millikan (LM) graph for (9,0) CNT - biphenyl – p-doped (8,0) CNT. The points labeled by circles correspond to voltages where negative diferential conductance and resonances occur.

Figure 3 shows that FN and ML graphs exhibit different values of resonance and NDR. The current-voltage characteristics (I-V) and the normalized conductance-voltage (G/G_0-V) curve are shown in Fig. 4. The resonance and NDR can be better identified in Fig. 3(a), presenting strong coupling in this junction for same applied bias. However, when the NDR shows up, the coupling changes from strong to weak[22]. When the HOMO level crosses the Fermi level E_F a resonance occurs; when the LUMO level crosses the Fermi level a NDR occurs. These situations correspond to transmission peaks at $E \approx E_F$ in Fig. 5[17].

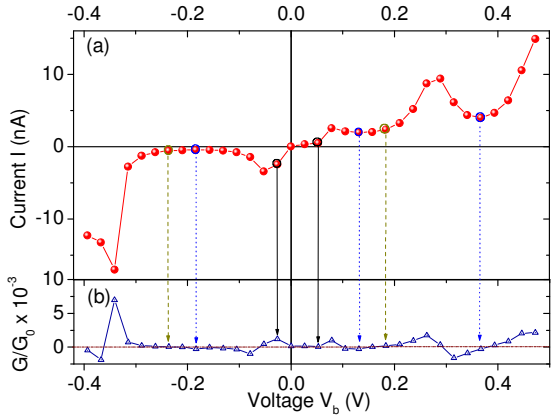

Fig. 4 (a) Current-voltage (I-V) and (b) normalized Conductance-voltage (G/G_0-V) curves for CNT (9,0) – biphenyl – p-doped CNT (8,0).

Figure 4 shows the asymmetric *(a)* current-voltage (I-V) and *(b)* differential conductance characteristics for the system investigated. Figure 5 exhibits the transmittance curves for different voltages for *(a)* reverse and *(b)* forward bias, respectively. In the following we pinpoint the major findings that can be inferred from these figures, together with Fig. 3: Negative applied bias: **(i)** at -0.026 V there is a resonance captured by the FN plot (Fig. 2), an increase in conductance [Fig. 4(b)], and transmittance centered in $E-E_F=0$ [Fig. 5(a)]; **(ii)** for -0.184 V negative differential resonance occurs, as the LM plot reveals

(Fig. 3), a decrease in conductance [Fig.3(b)], and transmittance centered in E-E_F=0 [Fig.5(a)]; **(iii)** for -0.236 V a resonance shows up, as it is clear from the FN plot (Fig.3), a small increase in conductance [Fig.4(b)] and transmittance centered at E-E_F=0 [Fig.5(a)]. Positive applied bias: **(iv)** a resonance, present at both LM and FN plots, occurs at 0.053 V (Fig.3), a small increase in conductance [Fig.4(b)] and transmittance centered in E=E_F [Fig.5(b)]; **(v)** negative differential resonance emerges at 0.131 V, as shown in the LM plot (Fig.3), a decrease in conductance

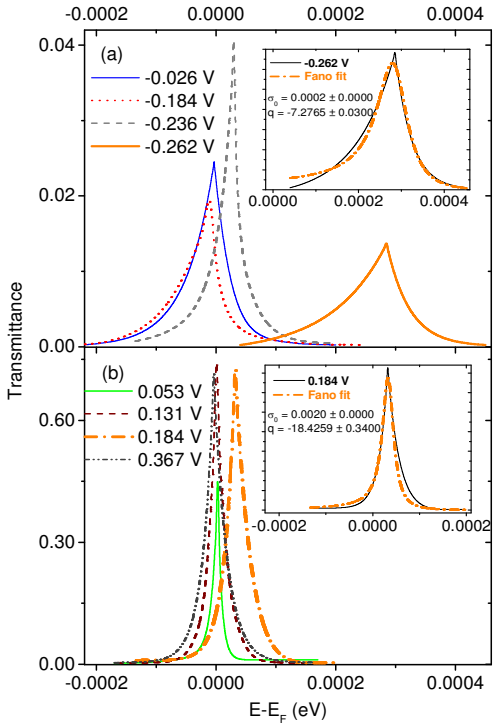

Fig. 5 Transmittance-energy barrier graph for different voltages in (a) reverse and (b) forward bias.

[Fig.4(b)], and transmittance centered at E-E_F=0 [Fig.5(b)]; **(vi)** negative differential resonance occurs for 0.184 V, as demonstrated by the FN plot (Fig.3), a small increase in conductance [Fig.4(b)] and transmittance not centered at E=E_F [Fig.5(b)]; **(vii)** at 0.367 V there is a region of negative differential resonance captured by both LM and FN (Fig.3) plots, a decrease in conductance [Fig.3(b)] and transmittance centered at E=E_F [Fig.5(b)].

The regions where NDR occurs are related to suppression in the current, suggesting that there is a crossover from strong to weak coupling[19] between the electrodes (CNT (9,0) and p-doped (8,0) CNT) and the molecular bridge (biphenyl). In a model where electronic transport can be described by a tunneling barrier, this crossover can be attributed to the fact that the Schottky barrier is very small in the p-doped CNT (8,0)-biphenyl junction. This behavior is asymmetric in the I-V curve because the left and right electrodes are metallic and semiconducting, respectively, so that the barrier height is different for reverse and forward bias. A similar result has been reported in the literature[11].

Figure 5 reveals that, for certain values of the applied voltage bias, the transmittance curves are asymmetric and cannot be described by the typical Lorentzian lineshape. Instead such curves are very well described by the Fano lineshape:

$$T(\varepsilon) = \sigma_0 \frac{(\varepsilon + q)^2}{1 + \varepsilon^2}, \qquad (2)$$

with ε=2(E-E_R)/Γ where E_R and Γ are position and width of the resonance, σ_o is normalized, and q is the asymmetry parameter (see inset of Fig.5). In general, the Fano effect in electronic transport results from the interference between the excited leaky modes in the central transport region (e.g. quantum dot, molecular bridge) and the incoming wavefunction from the electrodes[30]. In the present case, the fact that the transmittance curves are well described by the Fano lineshape suggests that the molecular frontier orbitals are being occupied during the transport process; since these states have a finite lifetime, they eventually leak and interfere with the incident wavefunction, resulting in the Fano asymmetric transmittance curves. This result supports the scenario in which the coherent transport model provides an adequate description of electronic transport in the molecular junctions under investigation, corroborating the current interpretation of transition voltage spectroscopy[31].

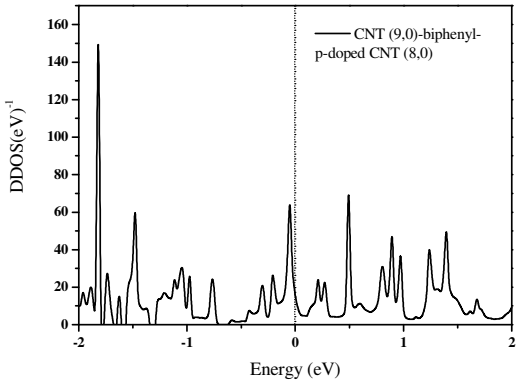

Fig. 6 The electronic density of states spectra (DDOS) for corresponding device presented in Figure 1. The dashed line indicate the Fermi level position.

Figure 6 shows the density of states (DDOS) for biphenyl derivative bridging the gap between single-wall (9,0) carbon nanotube and p-doped (8,0) carbon nanotube and it came from the imaginary contribution of retarded Green function in all molecular sites. The dashed line indicates the Fermi level position. The results indicate a conductor behavior with no energy gap for the considered configuration and the Fermi level is in the middle of band.

An inspection of Fig. 7 indicates that the HOMO surface is almost localized on the semiconductor NTC lead with small overlap in the first biphenyl atom. The LUMO state is delocalized on the left lead (metallic NTC) phenyl showing strong coupling (the pi orbitals overlap between electrode and molecule) when compared with right electrode.

Conclusions

We investigate electronic transport in semiconductor-molecule-metal junctions consisting of a biphenyl molecule attached to p-doped semiconductor and metallic carbon nanotubes. The fact that right and left leads have different electronic properties (metallic and semiconductor) is at the origin of interesting electronic transport phenomena. Indeed, we find that the current-voltage characteristics are asymmetric. Also we provide an analysis of transition voltage spectroscopy in such system by means of both Fowler-Nordheim and Lauritsen-Millikan plots; this analysis allows one to identify the positions of resonances and the regions where the negative differential conductance occurs. We demonstrate that transmittance curves are well described by the Fano lineshape, for both direct and reverse bias. This result suggests that the frontier molecular orbitals are effectively involved in the transport process, corroborating the coherent transport model in single-molecule electronics. By unveiling the connection between Fano resonances and transition voltage spectroscopy, we provide a novel way to understand and interpret Fowler-Nordheim plots, largely used in single-molecule electronics.

Acknowledgments

This work was partially supported by the Brazilian agencies CNPq, CAPES, FAPERJ, VALE/FAPESPA, Rede Nanotubos de Carbono/CNPq, INCT Nanomateriais de Carbono/CNPq, and ELETROBRÁS/ELETRONORTE. CABSJR and VFPA are grateful to UFPA/PROPESP/PARD project and CENAPAD-SP for computational support. CABSJR acknowledges Mr. J.A. Rodrigues-Neto and Mr. M.E.S. Sousa for fruitful discussions.

References

1 A. Aviran and M. Ratner, *Chem. Phys. Lett.*, 1974, **29**, 277-283.
2 R. L. McCreery, *Chem. Mater.*, 2004, **16**, 4477-4496.
3 M. M. Saitner, F. Eberle, J. Baccus, M. D'Olieslaeger, P. Wagner, D. M. Kolb and H. G. Boyen, *The J. of Phys. Chem. C*, 2012, **116**, 21810-21815.
4 J. J. Kushmerick, S. K. Pollack, J. C. Yang, J. Naciri, D. B. Holt, M. A. Ratner and R. Shashidhar, Ann. N.Y. Acad. Sci. 2003, **1006**, 277-290.
5 H. Nakayama and S. Kimura, *Chem. Phys. Lett.*, 2011, **508**, 281-284.
6 R. M. Metzger, Bo Chen, Ulf Höpfner, M. V. Lakshmikantham, D. Vuillaume, T. Kawai, X. Wu, H. Tachibana, T. V. Hughes, H. Sakurai, J. W. Baldwin, C. Hosch, M. P. Cava, L. Brehmer and G. J. Ashwell, *J. Am. Chem. Soc.*, 1997, **119**, 10455-10466.
7 S. Hong, R. Reifenberger, W. Tian, S. Datta, J. I. Henderson and C. P. Kubiak, *Superlatt. and Microstruc.*, 2000, **28**, 289-303.
8 A. Nitzan and M. A. Ratner, *Science*, 2003, **300**, 1384-1389.
9 F. Börrnert, C. Börrnert, S. Gorantla, X. Liu, A. Bachmatiuk, J.-O. Joswig, F. R. Wagner, F. Schäffel, J. H. Warner, R. Schönfelder, B. Rellinghaus, T. Gemming, J. Thomas, M. Knupfer, B. Büchner and M. H. Rümmeli, *Phys. Rev. B*, 2010, **81**, 0854391-0854395.
10 T. Albrecht, *Nat. Commun.*, 2012, **3**, 829-839.
11 A. Salomon, T. Boecking, O. Seitz, T. Markus, F. Amy, C. Chan, W. Zhao, D. Cahen and A. Kahn, *Adv. Mater.*, 2007, **19**, 445-450.
12 L. H. Yu, N. Gergel-Hackett, C. D. Zangmeister, C. A. Hacker, C. A. Richter and J. G. Kushmerick, *J. of Phys.: Cond. Matt.*, 2008, **20**, 3741141-3741145.
13 R. M. Metzger, *J. Mater. Chem.*, 2008, **18**, 4364-4396.
14 J. M. Beebe, B. Kim, J. W. Gadzuk, C. D. Frisbie and J. G. Kushmerick, *Phys. Rev. Lett.*, 2006, **97**, 0268011-0268014.
15 J. M. Beebe, B. Kim, C. D. Frisbie and J. G. Kushmerick, *ACS Nano*, 2008, **2**, 827-832.
16 N. A. Bruque, M. K. Ashraf, G. J. O. Beran, T. R. Helander and R. K. Lake, *Phys. Rev. B*, 2009, **80**, 1554551-15545513.
17 C. A. B. Silva Jr., S. J. S. da Silva, E. R. Granhen, J. F. P. Leal, J. Del Nero and F. A. Pinheiro, *Phys. Rev. B*, 2010, **82**, 0854021-0854025.
18 A. D. J. Becke, *Chem. Phys.*, 1993, **98**, 1372-1377; J. P. Perdew, M. Ernzerhof and K. Burke, *J. Chem. Phys.*, 1996, **105**, 9982-9985; A. D. Becke, *Phys. Rev. A*, 1988, **38**, 3098-3100; S. H. Vosko, L. Wilk and M. Nusair, *J. Phys.*, 1980, **58**, 1200-1211.
19 W. Y. Kim, S. K. Kwon and K. S. Kim, *Phys. Rev. B*, 2007, **76**, 0334151-0334154.
20 A. Saraiva-Souza, R. M. Gester, M. A. Reis, F. M. Souza, J. Del Nero, *J. Comput. Theor. Nanosci.*, 2008, **5**, 2243-2246; A. Saraiva-Souza, F. M. Souza, V. F. P. Aleixo, E. C. Girao, Filho J. Mendes, V. Meunier, B. G. Sumpter, A. G. Souza Filho and J. Del Nero, *J. Chem. Phys.*, 2008, **129**, 204701-204704.
21 M. Brandbyge, J.-L. Mozos, P. Ordejón, J. Taylor, and K. Stokbro, *Phys. Rev. B*, 2002, **65**, 165401-165417.
22 K. Stokbro, J. Taylor and M. Brandbyge, *J. Am. Chem. Soc.*, 2003, **125**, 3674-3675; J. Taylor, M. Brandbyge and K. Stokbro, *Phys. Rev. Lett.*, 2002, **89**, 138301-138301; Z. K. Qian, S. M. Hou, R. Li, Z. Y. Shen, X. Y. Zhao, Z. Q. Xue, *J. Comput. Theor. Nanosci.*, 2008, **5**, 671-676.
23 S. U. Lee, M. Khazaei, F. Pichierri, and Y. Kawazoea, *Physical Chemistry Chemical Physics,* 2008, **10**, 5225–5231.
24 X. D. Cui, A. Primak, X. Zarate, J. Tomfohr, O. F. Sankey, A. L. Moore, T. A. Moore, D. Gust, L. A. Nagahara and S. M. Lindsay, *J. Phys. Chem. B*, 2002, **106**, 8609-8614.
25 R. Landauer, *IBM J. Res. Dev.*, 1957, **1**, 1-223; M. Büttiker, *Phys. Rev. Lett.*, 1986, **57**, 1761-1764.
26 A. Hernández, V. M. Apel, F. A. Pinheiro and C. H. Lewenkopf, *Physica A*, 2007, **385**, 148-160.
27 S. Datta, Quantum transport: Atom to transistor. Cambridge University Press, **2005**.
28 M. Tsukada and M. Airaidai, *Phys. Rev. B*, 2010, **81**, 2351141-2351147.
29 R. G. Forbes, *J. of Appl. Phys.*, 2009, **150**, 1143131-1143138.
30 A. E. Miroshnichenko, S. Flach and Y. Kivshar, *Rev. Mod. Phys.*, 2010, **82**, 2257-2298.

LUMO

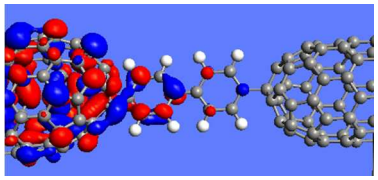

HOMO

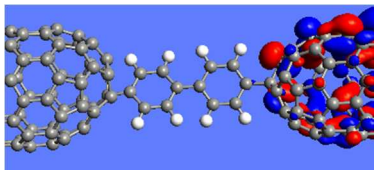

Fig. 7 LUMO and HOMO, respectively, for the investigated system with no applied bias.

31 E. H. Huisman, C. M. Guedon, B. J. van Wees and S. J. van der Molen, *Nano Lett.*, 2009, **9**, 3909-3913.

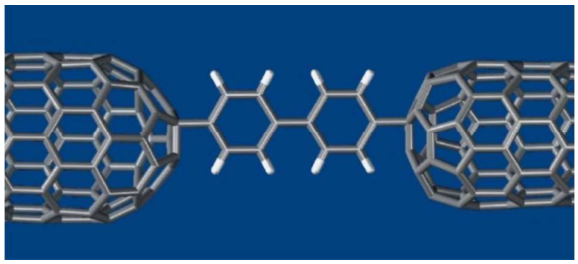

We investigate electronic transport in semiconductor-molecule-metal junctions consisting of a biphenyl molecule attached to p-doped semiconductor and metallic carbon nanotubes.